HHS Public Access

Author manuscript

J Am Chem Soc. Author manuscript; available in PMC 2019 January 28.

Published in final edited form as:

J Am Chem Soc. 2018 October 31; 140(43): 14087–14096. doi:10.1021/jacs.8b05530.

Self-Assembly of Supramolecular Fractals from Generation 1 to 5

Lei Wang[†,¶], **Ran Liu**[‡,§,¶], **Jiali Gu**[‖], **Bo Song**[†], **Heng Wang**[†], **Xin Jiang**[⊥], **Keren Zhang**[§], **Xin Han**[#], **Xin-Qi Hao**[#], **Shi Bai**[▽], **Ming Wang**[⊥], **Xiaohong Li**[‖], **Bingqian Xu**[§], and **Xiaopeng Li**[†]

[†]Department of Chemistry, University of South Florida, Tampa, Florida 33620, United States

[‡]Shandong Province Key Laboratory of Medical Physics and Image Processing Technology, School of Physics and Electronics, Shandong Normal University, Jinan 250358, China

[§]Single Molecule Study Laboratory, College of Engineering and Nanoscale Science and Engineering Center, University of Georgia, Athens, Georgia 30602, United States

[‖]College of Chemistry, Chemical Engineering and Materials Science, Soochow University, Suzhou 215123, China

[⊥]State Key Laboratory of Supramolecular Structure and Materials, College of Chemistry, Jilin University, Changchun, Jilin 130012, China

[#]College of Chemistry and Molecular Engineering, Zhengzhou University, Zhengzhou, Henan 450001, China

[▽]Department of Chemistry and Biochemistry, University of Delaware, Newark, Delaware 19716, United States

Abstract

In the seeking of molecular expression of fractal geometry, chemists have endeavored in the construction of molecules and supramolecules during the past few years, while only a few examples were reported, especially for the discrete architectures. We herein designed and constructed five generations of supramolecular fractals (**G1−G5**) based on the coordination-driven self-assembly of terpyridine ligands. All the ligands were synthesized from triphenylamine motif, which played a central role in geometry control. Different approaches based on direct Sonogashira coupling and/or ⟨tpy-Ru(II)-tpy⟩ connectivity were employed to prepare complex Ru(II)-organic building blocks. Fractals **G1−G5** were obtained in high yields by precise coordination of organic or Ru(II)-organic building blocks with Zn(II) ions. Characterization of those architectures were accomplished by 1D and 2D NMR spectroscopy, electrospray ionization mass spectrometry (ESI-MS), traveling-wave ion mobility mass spectrometry (TWIM-MS), and transmission electron

Correspondence to: Ming Wang; Xiaohong Li; Bingqian Xu; Xiaopeng Li.

[¶]L.W. and R.L. contributed equally.

Supporting Information

The Supporting Information is available free of charge on the ACS Publications website at DOI: 10.1021/jacs.8b05530.

Synthetic details, ligands and complexes characterization including ^{1}H NMR, ^{13}C NMR, 2D COSY, 2D NOESY, ESI-MS, TWIM-MS, UV−vis, CV, TEM and STM images (PDF)

The authors declare no competing financial interest.

microscopy (TEM). Furthermore, the two largest fractals also hierarchically self-assemble into ordered supramolecular nanostructures either at solid/liquid interface or in solution on the basis of their well-defined scaffolds.

Graphical Abstract

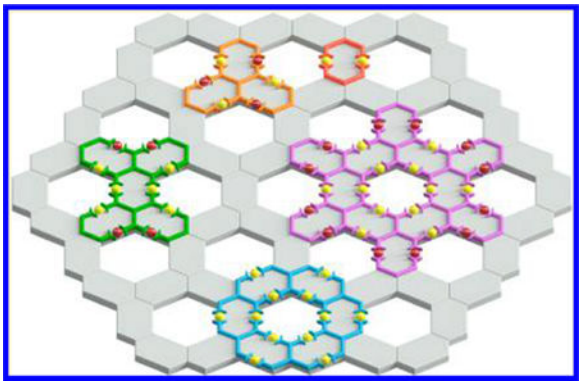

INTRODUCTION

The concept of “fractal geometry” is coined by Mandelbrot to describe the natural geometries, which cannot be described precisely using ideal constructions of Euclidean geometry, such as lines, triangles, squares, circles, spheres, etc.[1] As an important characteristic, fractal geometry displays self-similarity at different levels of magnification. Inspired by nature and mathematics, the fractal geometry was introduced into several different scientific fields from physics to geo-morphology, from chemistry to materials science, and from economics to biology.[2] In particular, the fractal geometry has been behind an enormous change in the way chemists perceive, and subsequently rebuild, the chemistry field in which we explore.[3,4] For instance, dendrimers have been extensively demonstrated to be iconic molecular fractals in conventional synthetic chemistry.[5–10]

In the seeking of alternatives to avoid multistep synthesis, surface self-assembly recently was employed to construct a well-known fractal geometry, viz., Sierpiński triangle,[11] through theoretical prediction,[12] halogen bonding,[13] hydrogen bonding[14] and coordination[15–17] in ultrahigh vacuum. However, different generations of fractals were assembled as a mixture on the surface. With the goal of exerting more elegant manipulation over structural features of fractals, coordination-driven supramolecular chemistry has stepped into the construction of discrete metallo-supramolecular Sierpiński triangles[18,19] and gaskets[20] through the self-assembly in solution with high yields. Although metallo-supramolecular chemistry has witnessed a spectacular explosion in constructing a great variety of polygons and polyhedrons in the field of Euclidean geometry,[21–37] it still remains a formidable challenge to assemble nontrivial architectures, particularly high generation of fractals. Up to date, most of these metallo supramolecular fractals are limited to low generation of (≤3) Sierpiński geometry (Figure 1a) due to the challenge of design, synthesis and separation. An important question was raised: can one assemble other high generations of supramolecular fractals rather than Sierpiński fractals?

In this study, we used well-documented 2,2′:6′,2″-terpyridine (tpy)-based coordination chemistry[38–48] to construct discrete supramolecular fractals ranging from generation 1 (**G1**) to 5 (**G5**) in high yields. Except for **G1** and **G4**, all other fractals were assembled using two combinations of connectivity, i.e., ⟨tpy-Ru(II)-tpy⟩ and ⟨tpy-Zn(II)-tpy⟩. Briefly, a series of Ru(II)-organic building blocks (ROBBs) was synthesized on the basis of the strong binding ability between tpy and Ru(II).[49–51] In the following self-assembly, such ROBBs can assemble with weak coordination metal, i.e., Zn(II) to construct **G2, G3** and **G5** fractals with increasing size and complexity. More importantly, these architectures exhibit fractal characteristics through repeating the basic shape unit (**G1**) to form branched frameworks. It is worth noting that supramolecular fractals we reported here display only statistical self-similarity, which are not identical at all levels of magnification (Figure 1b). By contrast, computer generated (i.e., mathematical) fractals can repeat their self-similarity at all scales.

RESULTS AND DISCUSSION

In an effort to elaborate the concept of fractal by coordination-driven self-assembly, a series of ligands was designed with the goal of assembling a set of discrete structures with Zn(II) ions rather than infinite framework. Those structures possess the same repeating shape unit, namely **G1**, but display at different scales, leading to different molecular geometry and symmetry. **G2** contains three repeating units with a triangle geometry, while **G3** is comprised of five repeating units with a dumbbell-shaped geometry. The higher generations **G4** and **G5** consist of 6 and 12 repeating units, respectively. Moreover, all the geometry of **G1** to **G4** can be found as a proportion in **G5**, which exhibits the extended supramolecular fractal with high complexity. According to molecular modeling, the size is enlarged more than four times from the smallest supramolecule **G1** (~2.5 nm) to the largest one **G5** (~11 nm) (Figure 2).

In our synthetic design, triphenylamine motifs played a central role in controlling the geometry of assemblies due to their specific internal bond angles with appropriate molecular rigidity.[52] Tpy units, which were widely used in coordination-driven self-assembly,[43–52] were introduced to provide coordination sites for metal ions. Considering the accessibility, three approaches were utilized to construct building blocks. Approach 1 was using Sonogashira coupling reaction to connect the triphenylamine motifs and tpy directly, for instance, organic ligands **LA** and **LD** (Scheme 1). Approach 2 was bridging two organic tpy ligands using Ru(II) chemistry to form ROBB, such as **LE** with increasing complexity and avoiding multiple self-assembly products.[49a,50] Approach 3 was a combination of the first two methods through performing Sonogashira coupling on the Ru(II)-tpy complexes to precisely control the structures of ligands and the self-assembly supramolecules as well as increasing the diversity and complexity, such as **LB** and **LC**. Note that the ⟨tpy− Ru(II)−tpy⟩ connectivity was able to sustain the basic condition and high temperature in the cross-coupling reaction due to its high stability.[49a]

Synthesis of Ligands and Fractals.

We initiated the ligand synthesis from organic ligands **L** and **LA**, which were obtained easily by approach 1 through connecting different triphenylamine motifs and tpy units using

Sonogashira coupling (Schemes S2 and S5). **L** was designed to provide scaffolds of the higher generations of fractals, while **LA** was able to end-cap the outer binding sites to prevent the formation of infinite structure. **LA** itself could self-assemble into complex [$\mathbf{Zn_2LA_2}$] in a stoichiometric ratio (1:1) with $Zn(NO_3)_2{\cdot}6H_2O$, resulting in the formation of the smallest structure **G1**, which represented the basic repeating shape unit in the complex fractal set. Electrospray ionization−mass spectrometry (ESI-MS) and traveling wave ion mobility mass spectrometry (TWIM-MS)[53–56] provided strong evidence for the formation of **G1** with a molecular weight of 2722 Da (Figure S8). ^{1}H NMR, 2D COSY (correlation spectroscopy), and 2D NOESY (nuclear Overhauser effect spectroscopy) spectra supported the formation of the symmetrical structure (Figures S76–S81).

In the assembly of **G2**, we initially designed **LB′** through end-capping **L** with three equivalents of **LA** (Figure S1). However, no desired product was achieved after vigorous efforts due to the inert coordination of Ru(II). Therefore, we redesigned and synthesized **LB** using approach 3 to overcome the inertness of coordination with the combination of Sonogashira coupling reaction and Ru(II) chemistry. Ironically, **LB** with three Ru(II) ions and six free tpy groups is the most challenging one among all the building blocks for the fractals, although **G2** is a relatively small structure among those five fractals.

Two steps of Sonogashira coupling were performed on the Ru(II)-tpy complex **S-18** to control the structure of the target ligand and assembled supramolecule (Scheme S3). Complex [$\mathbf{Zn_3LB}$] or fractal **G2** with three repeating units was then obtained by assembling **LB** with Zn(II) in a 1:3 ratio, followed by the counterions exchange from NO_3^- to PF_6^- for mass spectrometry characterization. Note that **G2** was not accessible through direct mixing **L** and **LA** in 1:3 ratio with corresponding Zn(II) because of self-sorting of individual building block.

In the design of **G3**, the preparation of **LC′** was unsuccessful using approach 2 because of the inert coordination of Ru(II) (Figure S1). As such **LC** was synthesized using the same strategy as **LB** but underwent only one step of Sonogashira coupling on ROBB as shown in Scheme S4. Briefly, **LC** was prepared through coupling of organic precursor **S-13** and Ru(II)-tpy complex **S-21**, which was obtained via double end-capping of precursor **S-8** with **LA** and Ru(II). Such combination strategy allowed us to prepare **LC** in a moderate isolation yield after a column chromatography separation. Complex [$\mathbf{Zn_6LC_2}$] or fractal **G3** was obtained in a yield of 94% by mixing **LC** and $Zn(NO_3)_2{\cdot}6H_2O$ in a 1:3 ratio, followed by the same treatment as the other fractals. **G3** is comprised of 5 repeating units with 2 organic precursor compound **L** and 4 **LA** in each structure; similarly, the direct self-assembly of **L** and **LA** in 1:2 ratio with corresponding Zn(II) was unable to form **G3**-like fractal because of the self-sorting of individual building block.

ESI-MS and TWIM-MS spectra provided structural information on **G2** and **G3** with one set of multiple charged signals observed from 1D ESI-MS and 2D TWIM-MS spectra. Corresponding isotope pattern of each charged state agreed well with theoretical one (Figures 3 and 4). ^{1}H NMR spectra, 2D COSY and 2D NOESY spectra of ligand **LB** and fractal **G2** showed four types of tpy (Figure S106). ^{1}H NMR spectra showed four types of

tpy for Ligand **LC** but five types of tpy for fractal **G3** (Figure S107). The assigned structures were supported by detailed 2D COSY and 2D NOESY spectra (Figures S82−S93).

Organic ligand **LD** was obtained in a straightforward manner by approach 1 through direct Sonogashira coupling. The organic ligand could form the complex [$\mathbf{Zn_{12}LD_6}$], or **G4** in the fractal set, with $Zn(NO_3)_2{\cdot}6H_2O$ in a 1:2 ratio. ESI-MS and TWIM-MS spectra provided strong evidence for the formation of **G4** with molecular weight of 14865 Da. Only one prominent set of signals for multicharged signals (from 10+ to 19+) was observed in ESI-MS spectrum (Figure 5a). Moreover, a narrow distribution of drift time for different charge states in TWIM-MS spectrum (Figure 5b) indicated there were no isomers or structural conformers generated. Furthermore, the isotope pattern of the multicharged ions agreed well to the simulated one, suggesting the proposed structure (Figure S12). ^{1}H NMR, 2D COSY and 2D NOESY spectra (Figures S96−S99) supported the formation of symmetrical structures. For instance, in the ^{1}H NMR spectrum of **G4**, two types of tpy units were observed and the resonance signals had distinguishable shift compared to **LD** (Figure 6).

The synthesis of **LE** was achieved by approach 2 through end-capping hexatopic tpy ligand **L** with one **LA** using Ru(II) chemistry in two steps (Scheme 2). Such end-capping approach left four free tpy moieties for further coordination. Complex [$\mathbf{Zn_{12}LE_6}$] (i.e., **G5**), the largest supramolecule in the fractal set was obtained in high yield (96%) by treatment **LE** with $Zn(NO_3)_2{\cdot}6H_2O$ in a stoichiometric ratio (1:2) in $CHCl_3$/MeOH (v/v 1:3) at 50 °C for 10 h, followed by counterion exchange. ESI-MS and TWIM-MS spectra identified the formation of desired fractal **G5** with molecular weight of 28 384 Da. Also, one prominent set of signals was observed for multicharged signals (from 14+ to 28+) in ESIMS spectrum (Figure 7a) and TWIM-MS spectrum (Figure 7b) as other fractals did. ^{1}H NMR spectra of **LE** and **G5** were consistent with the assigned structure. Four sets of tpy signals were observed in both ligand and complex, indicating a highly symmetrical structure was formed after complexation (Figure 8). All the protons of 3′, 5′ positions on the metal-free tpy units of **LE**, i.e., $A^{3',5'}$ and $B^{3',5'}$ were shifted downfield (~0.4 ppm) due to electron deficiency upon coordination with metal ions, while those protons of 6, 6″ positions were significantly shifted upfield (~0.7 ppm) due to electron shielding effects according to the previous reports.[45a,50] In addition, the characteristic protons on alkoxy chain (−OCH_2−) with a 1:2:1 integration ratio also suggested the formation of discrete structure rather than polymers. All the assignments were confirmed by detailed 2D COSY and 2D NOESY spectra, respectively (Figures S102−S105).

Diffusion-ordered NMR spectroscopy (DOSY) experiments were conducted to provide dimensional information on those supramolecular assemblies.[48,57] All the five spectra showed narrow bands of signal that suggested the self-assemblies formed discrete supramolecular architectures (Figure 9). Moreover, the diffusion coefficient (D, m^2/s) decreased from 4.99×10^{-10} to 1.46×10^{-10} as the size gradually increased from **G1** to **G5**.[57,58] And the experimental hydrodynamic radius (r_H) of the fractals from the D value agreed well to the molecular modeling. For instance, the obtained radii for **G4** and **G5** were 4.2 and 5.7 nm, respectively, which were comparable to the sizes obtained from the modeling. And the results were summarized in Table S1.

Transmission electron microscopy (TEM) was also utilized to provide further structural information on the shape and size of the complexes, especially the large fractals **G4** and **G5**. The measured dimension of individual supramolecule deposited on the surface of copper grid showed the diameter around 7 and 12 nm (the average distance between the farthest corners) for **G4** and **G5**, respectively from TEM images (Figures 10a–d), which were also consistent with the sizes obtained from molecular dynamic modeling as well as DOSY NMR experiments.

Physical Properties.

Given that triphenylamine motifs and tpy-metal complexes were extensively studied for optoelectronic application,[52,59] a series of experiments was performed to study photophysical and electrochemical properties of the complexes. Absorption spectra for complexes are shown in Figure S112. All the complexes exhibited the typical $\pi \rightarrow \pi^*$ bands localized on the tpy-Ph subunits of ligands at around 285 and 325 nm because of intraligand charge transfer (^{1}ILCT). The band formed at around 485 nm in **G2, G3** and **G5** is assigned to the Ru(II)-tpy moiety because of the metal-to-ligand charge transfer (MLCT) transitions.[60] All the five fractals also show a characteristic absorption band centered at 390 nm, which corresponds to the intramolecular charge transfer transition from the triphenylamine motif to the tpy-metal component.[61,62]

Oxidation and reduction properties of all the five fractals were studied using cyclic voltammetry (CV), and the results were summarized in Figure S113. Two irreversible couples observed between −1.8 and −0.5 V are ascribed to the tpyligand-centered redox process, while overlapped by the broad peak from reduction process of triphenylamine motifs.[52] The Ru(II)/Ru(III) oxidation process of tpy-based complex occurred at 0.8−1.0 V according to the literature,[63] and the oxidation of the organic amine unit also occurred at around 1.0 and 1.2 V with broad peak corresponding to successive one electron removal.[64,65] That leads to an overlap in **G2, G3** and **G5** in the positive potential region.

Hierarchical Self-Assembly Behaviors.

We investigated the hierarchical self-assembly behaviors of fractals **G4** and **G5** under different conditions. TEM imaging showed that **G4** could further self-assemble into columnar nanostructures, which were bound together to form twisted fiber-like aggregates (Figure 11a) by diffusing THF into the solution of the complex (5 mg/mL in DMF) slowly. **G5** also hierarchically assembled into a well-organized tubular structure under the same condition and the diameter (~12 nm) of nanostructures was close to that of the individual fractal **G5** from energy-minimized structure by molecular modeling (Figure 11b). The formation of those ordered nanostructures were probably ascribed to the multiple intermolecular interactions such as $\pi-\pi$ stacking, CH$-\pi$ hydrophobic/hydrophilic interactions.[66] The proposed stacking models were displayed in Figures 11c and 11d. We speculated that the diameter and the orientation of the repeating units might result in the different hierarchical self-assembly behaviors of **G4** and **G5** in solution.

The hierarchical self-assembly behaviors of complexes **G4** and **G5** at liquid/solid interface were further investigated using scanning tunneling microscopy (STM). It is well-known that

molecules could self-assemble into ordered 2D materials at liquid/solid interface through noncovalent interactions such as intermolecular, molecule−substrate, molecule−solvent, solvent−substrate interactions.[67,68] However, giant metallo-supra-molecules were less explored because of the challenges in construction of large supramolecules with well-defined geometry. Furthermore, many previous studies reported that alkylated compounds tended to form ordered supramolecular assemblies on the highly oriented pyrolytic graphite (HOPG) surface due to their high affinities.[69,70] We herein reasoned that the giant complexes **G4** and **G5** with many alkyl chains on the rigid architectures could directly self-assemble into ordered 2D nanopattern on HOPG surface. Ambient STM imaging showed the formation of the anticipated honeycomb 2D supramolecular networks for both **G4** (Figures 12a, 12b, and 12d) and **G5** (Figures 12f, 12g, and 12i) after dropcasting of the fresh prepared solution onto HOPG surface. Obviously, the networks formed by **G4** had higher resolution, which might result from its higher rigidity compared to **G5**.

More interestingly, with short incubation time, 1D supra-molecular metal−organic nanoribbons (SMON)[58,71] with single-molecule width were also observed on HOPG surfaces (Figures 12e, 12h, and 12k). The SMON might grow along specific lattice direction of HOPG according to the reported gold(I) cyanide nanowires formed on graphene;[72] however, the current resolution by ambient STM was unable to provide more conclusive evidence. The achievements of those 2D networks and 1D orientated nanostructures on surfaces from giant supramolecular fractals might advance the study of surface chemistry for molecular-scale applications.[73,74]

CONCLUSIONS

In summary, five supramolecular architectures using triphenylamine and tpy moieties were successfully designed to demonstrate the concept of “supramolecular fractal”. In preparation of the ligands, different approaches were applied to precisely control the geometry as well as increasing the complexity. Particularly, the extensive utilization of Sonogashira coupling reaction on the Ru(II)-tpy complexes was able to significantly increase the complexity of building blocks, and thus substantially increased the diversity and complexity of metallo-supramolecules. With such strategy, we were able to construct nontrivial architectures, particularly high generation of fractals, which were not achievable using conventional direct self-assembly approach. Their photophysical and electro-chemical properties were investigated for further application study. Besides the self-assembly of the discrete structures, the hierarchical self-assembly of the largest fractals, **G4** and **G5** were also studied under different conditions. They were found to form tubular aggregates in solution while 2D networks and 1D orientated SMON on HOPG surface. Those unique hierarchical self-assembly behaviors of the giant supra-molecular architectures might broaden the avenue of novel materials such as semiconducting nanowires and 2D supra-molecular networks for specific applications at molecular level.

Supplementary Material

Refer to Web version on PubMed Central for supplementary material.

ACKNOWLEDGMENTS

The authors gratefully acknowledge the support from NSF (CHE-1506722 to X.L.; ECCS-1609788 to B.X.), NIH (1R01GM128037 to X.L.), and National Natural Science Foundation of China (No. 21528201 and 21305098), and the Program for Science & Technology Innovation Talents in Universities of Henan Province (17HASTIT004 to X.-Q.H.), Natural Science Foundation of Jilin Province (20180101297JC to M. W.).

REFERENCES

(1). Mandelbrot BB Fractals: Form, Chance and Dimension; W H Freeman and Co.: New York, 1977.

(2). Barnsley MF Fractals Everywhere; Morgan Kaufmann Publishers: Burlington, MA, 1993.

(3). Rothschild WG Fractals in Chemistry; John Wiley & Sons Ltd.: New York, 1998.

(4). Avnir D The Fractal Approach to Heterogeneous Chemistry: Surfaces, Colloids, Polymers; John Wiley & Sons Ltd.: New York, 1989.

(5). Newkome GR; Yao Z; Baker GR; Gupta VK; Micelles. J. Org. Chem 1985, 50, 2003.

(6). Tomalia DA; Baker H; Dewald J; Hall M; Kallos G; Martin S; Roeck J; Ryder J; Smith P Polym. J 1985, 17, 117.

(7). Hawker CJ; Fréchet JM J. J. Am. Chem. Soc 1990, 112, 7638.

(8). Tomalia DA; Naylor AM; Goddard WA, III Angew. Chem., Int. Ed. Engl 1990, 29, 138.

(9). Newkome GR; Moorefield CN; Vögtle DF Dendrimers and Dendrons: Concepts, Syntheses; Applications Wiley-VCH: Weinheim, Germany, 2001.

(10). Grayson SM; Fréchet JM J. Chem. Rev 2001, 101, 3819.

(11). Sierpiński WC R. Hebd. Seances Acad. Sci 1915, 160, 302.

(12). Nieckarza D; Szabelski P Chem. Commun 2014, 50, 6843.

(13). Shang J; Wang Y; Chen M; Dai J; Zhou X; Kuttner J; Hilt G; Shao X; Gottfried JM; Wu K Nat. Chem 2015, 7, 389. [PubMed: 25901816]

(14). Zhang X; Li N; Gu G-C; Wang H; Nieckarz D; Szabelski P; He Y; Wang Y; Xie C; Shen Z-Y; Lü J-T; Tang H; Peng L-M; Hou S-M; Wu K; Wang Y-F ACS Nano 2015, 9, 11909. [PubMed: 26502984]

(15). Li N; Zhang X; Gu G-C; Wang H; Nieckarz D; Szabelski P; He Y; Wang Y; Lü J-T; Tang H; Peng L-M; Hou S-M; Wu K; Wang Y-F Chin. Chem. Lett 2015, 26, 1198.

(16). Sun Q; Cai L; Ma H; Yuan C; Xu W Chem. Commun 2015, 51, 14164.

(17). Zhang X; Li N; Liu L; Gu G; Li C; Tang H; Peng L; Hou S; Wang Y Chem. Commun 2016, 52, 10578.

(18). Sarkar R; Guo K; Moorefield CN; Saunders MJ; Chrys W; Newkome GR Angew. Chem., Int. Ed 2014, 53, 12182.

(19). Jiang Z; Li Y; Wang M; Liu D; Yuan J; Chen M; Newkome GR; Sun W; Li X; Wang P Angew. Chem., Int. Ed 2017, 56, 11450.

(20). Newkome GR; Wang P; Moorefield CN; Cho TJ; Mohapatra PP; Li S; Hwang S-H; Lukoyanova O; Echegoyen L; Palagallo JA; Iancu V; Hla S-W Science 2006, 312, 1782. [PubMed: 16690820]

(21). (a)Chakrabarty R; Mukherjee PS; Stang PJ. Chem. Rev 2011, 111, 6810. [PubMed: 21863792] (b)Cook TR; Stang PJ Chem. Rev 2015, 115, 7001. [PubMed: 25813093] (c)Yan X; Cook TR; Wang P; Huang F; Stang PJ Nat. Chem 2015, 7, 342. [PubMed: 25803473] (d)Shi Y; Santos IS-M; Cao C; Cook TR; Stang PJ. Proc. Natl. Acad. Sci. U. S. A 2014, 111, 9390. [PubMed: 24979805]

(22). (a)Brown CJ; Toste FD; Bergman RG; Raymond KN. Chem. Rev 2015, 115, 3012. [PubMed: 25898212] (b)Pluth MD; Bergman RG; Raymond KN Science 2007, 316, 85. [PubMed: 17412953] (c)Zhao C; Sun Q-F; Hart-Cooper WM; DiPasquale AG; Toste FD; Bergman RG; Raymond KN J. Am. Chem. Soc 2013, 135, 18802. [PubMed: 24283463]

(23). (a)Harris K; Fujita D; Fujita M. Chem. Commun 2013, 49, 6703.(b)Sun Q-F; Iwasa J; Ogawa D; Ishido Y; Sato S; Ozeki T; Sei Y; Yamaguchi K; Fujita M Science 2010, 328, 1144. [PubMed: 20430973] (c)Fujita D; Ueda Y; Sato S; Mizuno N; Kumasaka T; Fujita M Nature 2016, 540, 563.

(24). (a)Smulders MMJ; Riddell IA; Browne C; Nitschke JR. Chem. Soc. Rev 2013, 42, 1728. [PubMed: 23032789] (b)McConnell AJ; Wood CS; Neelakandan PP; Nitschke JR Chem. Rev 2015, 115, 7729. [PubMed: 25880789] (c)Riddell IA; Hristova YR; Clegg JK; Wood CS; Breiner B; Nitschke JR J. Am. Chem. Soc 2013, 135, 2723. [PubMed: 23343477]

(25). (a)Ayme J-F; Beves JE; Leigh DA; McBurney RT; Rissanen K; Schultz DA. Nat. Chem 2012, 4, 15.(b)Danon JJ; Krüger A; Leigh DA; Lemonnier J-F; Stephens AJ; Vitorica-Yrezabal IJ; Woltering SL Science 2017, 355, 159. [PubMed: 28082585]

(26). (a)Han M; Engelhard DM; Clever GH. Chem. Soc. Rev 2014, 43, 1848. [PubMed: 24504200] (b)Frank M; Ahrens J; Bejenke I; Krick M; Schwarzer D; Clever GH J. Am. Chem. Soc 2016, 138, 8279. [PubMed: 27258549]

(27). (a)Lehn J-M. Chem. Soc. Rev 2007, 36, 151. [PubMed: 17264919] (b)Hasenknopf B; Lehn J-M; Boumediene N; Dupont-Gervais A; van Dorsselaer A; Kneisel B; Fenske DJ Am. Chem. Soc 1997, 119, 10956.(c)Barboiu M; Vaughan G; Graff R; Lehn J-MJ Am. Chem. Soc 2003, 125, 10257.

(28). (a)Ayme J-F; Beves JE; Leigh DA; McBurney RT; Rissanen K; Schultz DA. Nat. Chem 2012, 4, 15.(b)Danon JJ; Krüger A; Leigh DA; Lemonnier J-F; Stephens AJ; Vitorica-Yrezabal IJ; Woltering SL Science 2017, 355, 159. [PubMed: 28082585]

(29). Dalgarno SJ; Power NP; Atwood JL Coord. Chem. Rev 2008, 252, 825.(b)Fowler DA; Rathnayake AS; Kennedy S; Kumari H; Beavers CM; Teat SJ; Atwood JL. J. Am. Chem. Soc 2013, 135, 12184. [PubMed: 23909241]

(30). (a)Hargrove AE; Nieto S; Zhang T; Sessler JL; Anslyn EV. Chem. Rev 2011, 111, 6603. [PubMed: 21910402] (b)He Q; Tu P; Sessler JL Chem 2018, 4, 46. [PubMed: 29629424] (c)Hirao T; Kim DS; Chi X; Lynch VM; Ohara K; Park JS; Yamaguchi K; Sessler JL Nat. Commun 2018, 9, 823. [PubMed: 29483505]

(31). (a)Ward MD; Raithby PR. Chem. Soc. Rev 2013, 42, 1619. [PubMed: 22797247] (b)Würthner F; You C-C; Saha-Möller CR. Chem. Soc. Rev 2004, 33, 133. [PubMed: 15026818] (c)Qi Z; Heinrich T; Moorthy S; Schalley CA. Chem. Soc. Rev 2015, 44, 515. [PubMed: 24956973]

(32). (a)Mukherjee S; Mukherjee PS. Chem. Commun 2014, 50, 2239.(b)Bhat IA; Samanta D; Mukherjee PS J. Am. Chem. Soc 2015, 137, 9497. [PubMed: 26161983] (c)Kumar BA; Srinivasarao R; Dohyun M; Mukherjee PS. Chem. - Eur. J 2012, 18, 3199. [PubMed: 22314749]

(33). (a)Chen L-J; Yang H-B; Shionoya M. Chem. Soc. Rev 2017, 46, 2555. [PubMed: 28452389] (b)Hiraoka S; Yamauchi Y; Arakane R; Shionoya MJ Am. Chem. Soc 2009, 131, 11646.

(34). (a)Zhang GL; Zhou LP; Yuan DQ; Sun QF. Angew. Chem., Int. Ed 2015, 54, 9844.(b)Yan L-L; Tan C-H; Zhang G-L; Zhou L-P; Bünzli J-C; Sun Q-FJ Am. Chem. Soc 2015, 137, 8550. (c)Zhang T; Zhou L-P; Guo X-Q; Cai L-X; Sun Q-F Nat. Commun 2017, 8, 15898. [PubMed: 28621312]

(35). (a)Zhukhovitskiy AV; Zhong M; Keeler EG; Michaelis VK; Sun JEP; Hore MJA; Pochan DJ; Griffin RG; Willard AP; Johnson JA. Nat. Chem 2016, 8, 33. [PubMed: 26673262] (b)Wang Y; Gu Y; Keeler EG; Park JV; Griffin RG; Johnson JA Angew. Chem 2017, 129, 194.(c)Oldacre AN; Friedman AE; Cook TR J. Am. Chem. Soc 2017, 139, 1424. [PubMed: 28102678] (d)Preston D; Lewis JE; Crowley JD J. Am. Chem. Soc 2017, 139, 2379. [PubMed: 28110525]

(36). (a)Holliday BJ; Mirkin CA. Angew. Chem., Int. Ed 2001, 40, 2022.(b)Saalfrank RW; Maid H; Scheurer A Angew. Chem., Int. Ed 2008, 47, 8794.(c)Fasting C; Schalley CA; Weber M; Seitz O; Hecht S; Koksch B; Dernedde J; Graf C; Knapp E-W; Haag R Angew. Chem., Int. Ed 2012, 51, 10472.(d)Burke MJ; Nichol GS; Lusby PJ J. Am. Chem. Soc 2016, 138, 9308. [PubMed: 27351912] (e)Mirtschin S; Slabon-Turski A; Scopelliti R; Velders AH; Severin KJ Am. Chem. Soc 2010, 132, 14004.

(37). (a)Li J-R; Zhou H-C. Angew. Chem., Int. Ed 2009, 48, 8465.(b)Chen L-J; Ren Y-Y; Wu N-W; Sun B; Ma J-Q; Zhang L; Tan H; Liu M; Li X; Yang H-BJ Am. Chem. Soc 2015, 137, 11725. (c)Zheng W; Chen L-J; Yang G; Sun B; Wang X; Jiang B; Yin G-Q; Zhang L; Li X; Liu M; Chen G; Yang H-BJ Am. Chem. Soc 2016, 138, 4927.(d)Li K; Zhang L-Y; Yan C; Wei SC; Pan M; Zhang L; Su C-YJ Am. Chem. Soc 2014, 136, 4456.(e)Song B; Zhang Z; Wang K; Hsu CH; Bolarinwa O; Wang J; Li Y; Yin GQ; Rivera E; Yang HB; Liu C; Xu B; Li X Angew. Chem., Int. Ed 2017, 56, 5258.

(38). Schubert US; Eschbaumer C Angew. Chem., Int. Ed 2002, 41, 2892.

(39). Constable EC Chem. Soc. Rev 2007, 36, 246. [PubMed: 17264927]

(40). De S; Mahata K; Schmittel M Chem. Soc. Rev 2010, 39, 1555. [PubMed: 20419210]

(41). Wild A; Winter A; Schlütter F; Schubert US Chem. Soc. Rev 2011, 40, 1459. [PubMed: 21157599]

(42). Fermi A; Bergamini G; Roy M; Gingras M; Ceroni PJ Am. Chem. Soc 2014, 136, 6395.

(43). Zheng Z; Opilik L; Schiffmann F; Liu W; Bergamini G; Ceroni P; Lee L-T; Schütz A; Sakamoto J; Zenobi R; VandeVondele J; Schlüter AD J. Am. Chem. Soc 2014, 136, 6103. [PubMed: 24673195]

(44). Takada K; Sakamoto R; Yi S-T; Katagiri S; Kambe T; Nishihara HJ Am. Chem. Soc 2015, 137, 4681.

(45). (a)Chakraborty S; Newkome GR. Chem. Soc. Rev 2018, 47, 3991. [PubMed: 29594272] (b)Wang J-L; Li X; Lu X; Hsieh I-F; Cao Y; Moorefield CN; Wesdemiotis C; Cheng SZD; Newkome GR J. Am. Chem. Soc 2011, 133, 11450. [PubMed: 21657251] (c)Xie T-Z; Liao S-Y; Guo K; Lu X; Dong X; Huang M; Moorefield CN; Cheng SZD; Liu X; Wesdemiotis C; Newkome GR J. Am. Chem. Soc 2014, 136, 8165. [PubMed: 24840764] (d)Lu X; Li X; Guo K; Xie T-Z; Moorefield CN; Wesdemiotis C; Newkome GR J. Am. Chem. Soc 2014, 136, 18149. [PubMed: 25470035]

(46). (a)Fu J-H; Lee Y-H; He Y-J; Chan Y-T. Angew. Chem., Int. Ed 2015, 54, 6231.(b)Wang S-Y; Fu J-H; Liang Y-P; He Y-J; Chen Y-S; Chan Y-TJ Am. Chem. Soc 2016, 138, 3651.

(47). Chen M; Wang J; Liu D; Jiang Z; Liu Q; Wu T; Liu H; Yu W; Yan J; Wang PJ Am. Chem. Soc 2018, 140, 2555.

(48). (a)Wang M; Wang C; Hao X-Q; Li X; Vaughn TJ; Zhang Y-Y; Yu Y; Li Z-Y; Song M-P; Yang H-B; Li X. J. Am. Chem. Soc 2014, 136, 10499. [PubMed: 24978202] (b)Wang M; Wang C; Hao X-Q; Liu J; Li X; Xu C; Lopez A; Sun L; Song M-P; Yang H-B; Li XJ Am. Chem. Soc 2014, 136, 6664.(c)Wang L; Zhang Z; Jiang X; Irvin JA; Liu C; Wang M; Li X Inorg. Chem 2018, 57, 3548. [PubMed: 29166005]

(49). (a)Li Y; Jiang Z; Wang M; Yuan J; Liu D; Yang X; Chen M; Li X; Wang PJ. Am. Chem. Soc 2016, 138, 10041.(b)Jiang Z; Li Y; Wang M; Song B; Wang K; Sun M; Liu D; Li X; Yuan J; Chen M; Guo Y; Yang X; Zhang T; Moorefield CN; Newkome GR; Xu B; Li X; Wang P Nat. Commun 2017, 8, 15476. [PubMed: 28524876]

(50). Zhang Z; Wang H; Wang X; Li Y; Song B; Bolarinwa O; Reese RA; Zhang T; Wang X-Q; Cai J; Xu B; Wang M; Liu C; Yang H-B; Li XJ Am. Chem. Soc 2017, 139, 8174.

(51). Chakraborty S; Hong W; Endres KJ; Xie T-Z; Wojtas L; Moorefield CN; Wesdemiotis C; Newkome GR J. Am. Chem. Soc 2017, 139, 3012. [PubMed: 28165736]

(52). Hwang S-H; Moorefield CN; Wang P; Fronczek FR; Courtney BH; Newkome GR Dalton Trans 2006, 0, 3518.

(53). Chan Y-T; Li X; Yu J; Carri GA; Moorefield CN; Newkome GR; Wesdemiotis CJ Am. Chem. Soc 2011, 133, 11967.

(54). Brocker ER; Anderson SE; Northrop BH; Stang PJ; Bowers MT J. Am. Chem. Soc 2010, 132, 13486. [PubMed: 20815390]

(55). Scarff CA; Snelling JR; Knust MM; Wilkins CL; Scrivens JH J. Am. Chem. Soc 2012, 134, 9193. [PubMed: 22616687]

(56). Shi L; Holliday AE; Shi H; Zhu F; Ewing MA; Russell DH; Clemmer DE J. Am. Chem. Soc 2014, 136, 12702. [PubMed: 25105554]

(57). Yin G-Q; Wang H; Wang X-Q; Song B; Chen L-J; Wang L; Hao X-Q; Yang H-B; Li X Nat. Commun 2018, 9, 567. [PubMed: 29422628]

(58). Wang M; Wang K; Wang C; Huang M; Hao X-Q; Shen M-Z; Shi G-Q; Zhang Z; Song B; Cisneros A; Song M-P; Xu B; Li XJ Am. Chem. Soc 2016, 138, 9258.

(59). Tang J-H; Sun T-G; Shao J-Y; Gong Z-L; Zhong Y-W Chem. Commun 2017, 53, 11925.

(60). Schultz A; Li X; McCusker CE; Moorefield CN; Castellano FN; Wesdemiotis C; Newkome GR Chem. - Eur. J 2012, 18, 11569. [PubMed: 22907889]

(61). Robson KCD; Koivisto BD; Gordon TJ; Baumgartner T; Berlinguette CP Inorg. Chem 2010, 49, 5335. [PubMed: 20481435]

(62). Baitalik S; Wang X.-y.; Schmehl RH. J. Am. Chem. Soc 2004, 126, 16304. [PubMed: 15600315]
(63). Fan C; Ye C; Wang X; Chen Z; Zhou Y; Liang Z; Tao X Macromolecules 2015, 48, 6465.
(64). Xu X-D; Yao C-J; Chen L-J; Yin G-Q; Zhong Y-W; Yang H-B Chem. - Eur. J 2016, 22, 5211. [PubMed: 26771048]
(65). Yeh SJ; Tsai CY; Huang C-Y; Liou G-S; Cheng S-H Electrochem. Commun 2003, 5, 373.
(66). Ludlow JM; Saunders MJ; Huang M; Guo Z; Moorefield CN; Cheng SZD; Wesdemiotis C; Newkome GR Supramol. Chem 2017, 29, 69.
(67). Yang Y; Wang C Chem. Soc. Rev 2009, 38, 2576. [PubMed: 19690738]
(68). Kudernac T; Lei S; Elemans JAAW; De Feyter S Chem. Soc. Rev 2009, 38, 402. [PubMed: 19169457]
(69). Liu Y; Narita A; Teyssandier J; Wagner M; De Feyter S; Feng X; Müllen KA J. Am. Chem. Soc 2016, 138, 15539. [PubMed: 27934000]
(70). De Feyter S; De Schryver FC Chem. Soc. Rev 2003, 32, 139. [PubMed: 12792937]
(71). Wang H; Qian X; Wang K; Su M; Haoyang W-W; Jiang X; Brzozowski R; Wang M; Gao X; Li Y; Xu B; Eswara P; Hao X-Q; Gong W; Hou J-L; Cai J; Li X Nat. Commun 2018, 9, 1815. [PubMed: 29739936]
(72). Lee WC; Kim K; Park J; Koo J; Jeong HY; Lee H; Weitz DA; Zettl A; Takeuchi S Nat. Nanotechnol 2015, 10, 423. [PubMed: 25799519]
(73). Iritani K; Tahara K; De Feyter S; Tobe Y Langmuir 2017, 33, 4601. [PubMed: 28206764]
(74). Ammon M; Sander T; Maier SJ Am. Chem. Soc 2017, 139, 12976.

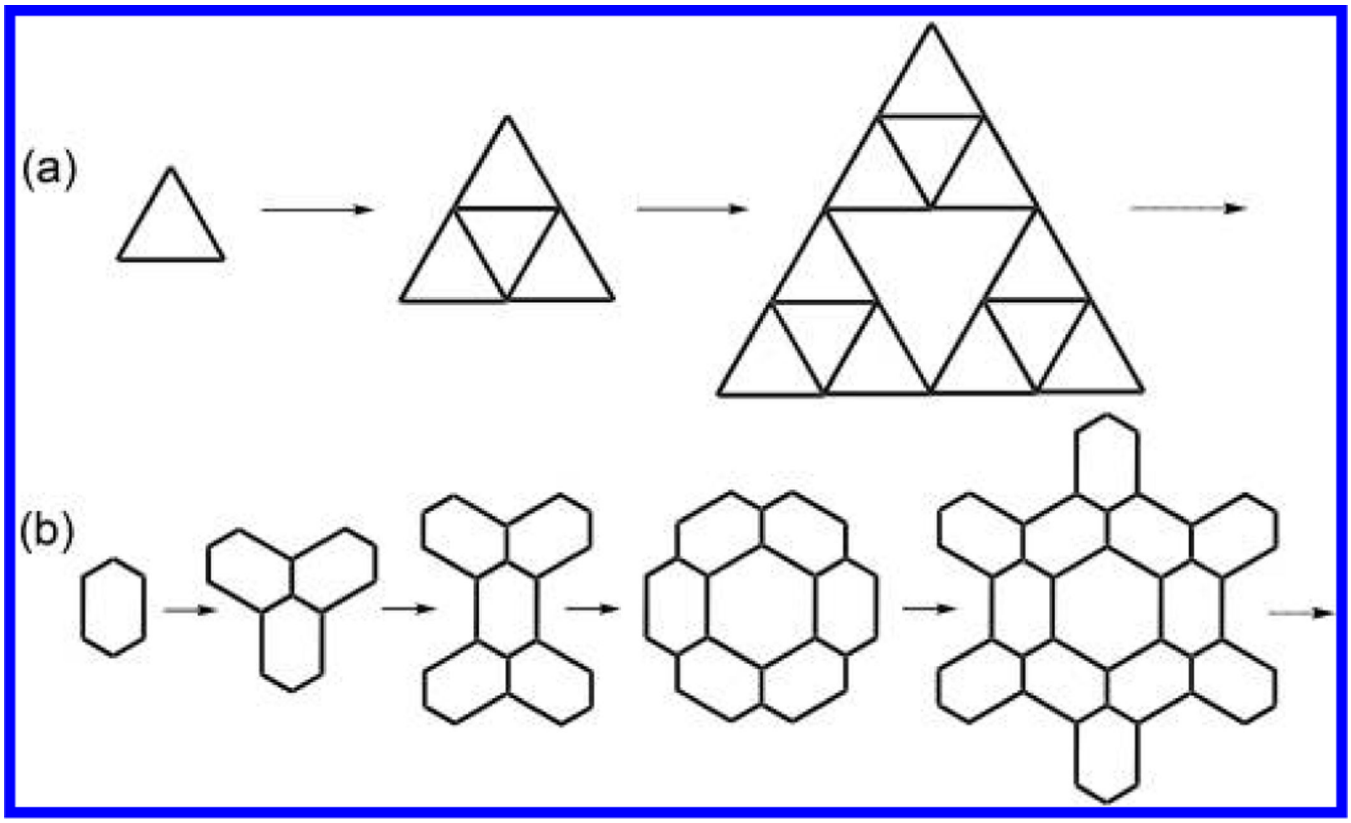

Figure 1.
(a) Sierpiński triangle fractals and (b) supramolecular fractals designed in this study.

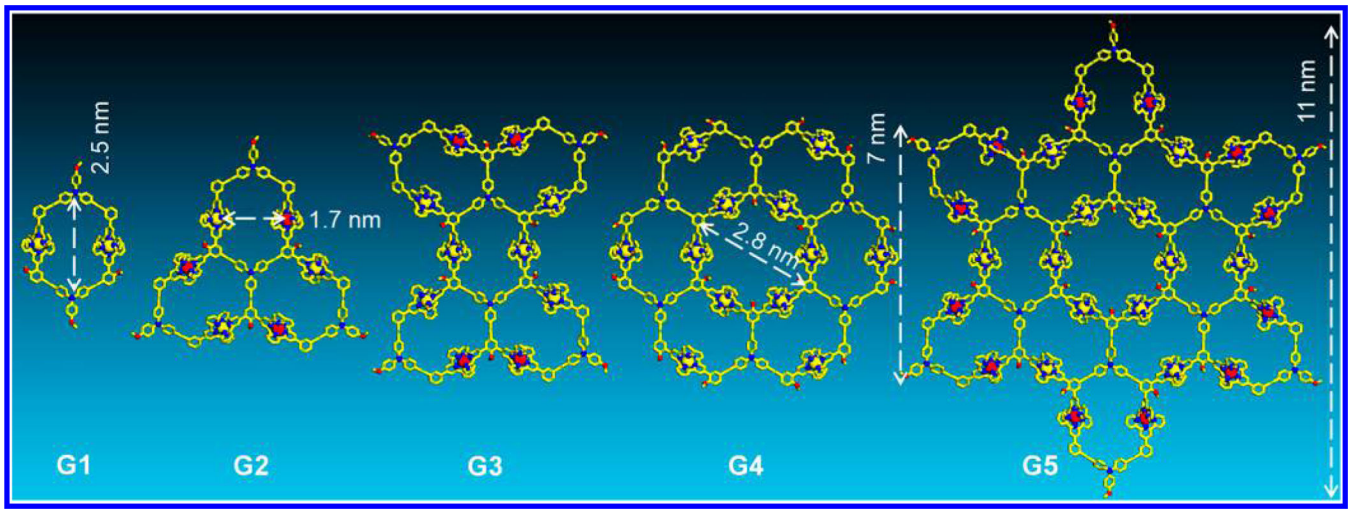

Figure 2.

Energy-minimized structures of fractal complexes **G1**[$\mathbf{Zn_2LA_2}$], **G2**[$\mathbf{Zn_3LB}$], **G3**[$\mathbf{Zn_6LC_2}$], **G4**[$\mathbf{Zn_{12}LD_6}$], **G5**[$\mathbf{Zn_{12}LE_6}$] from molecular modeling (the alkyl chains are omitted for clarity).

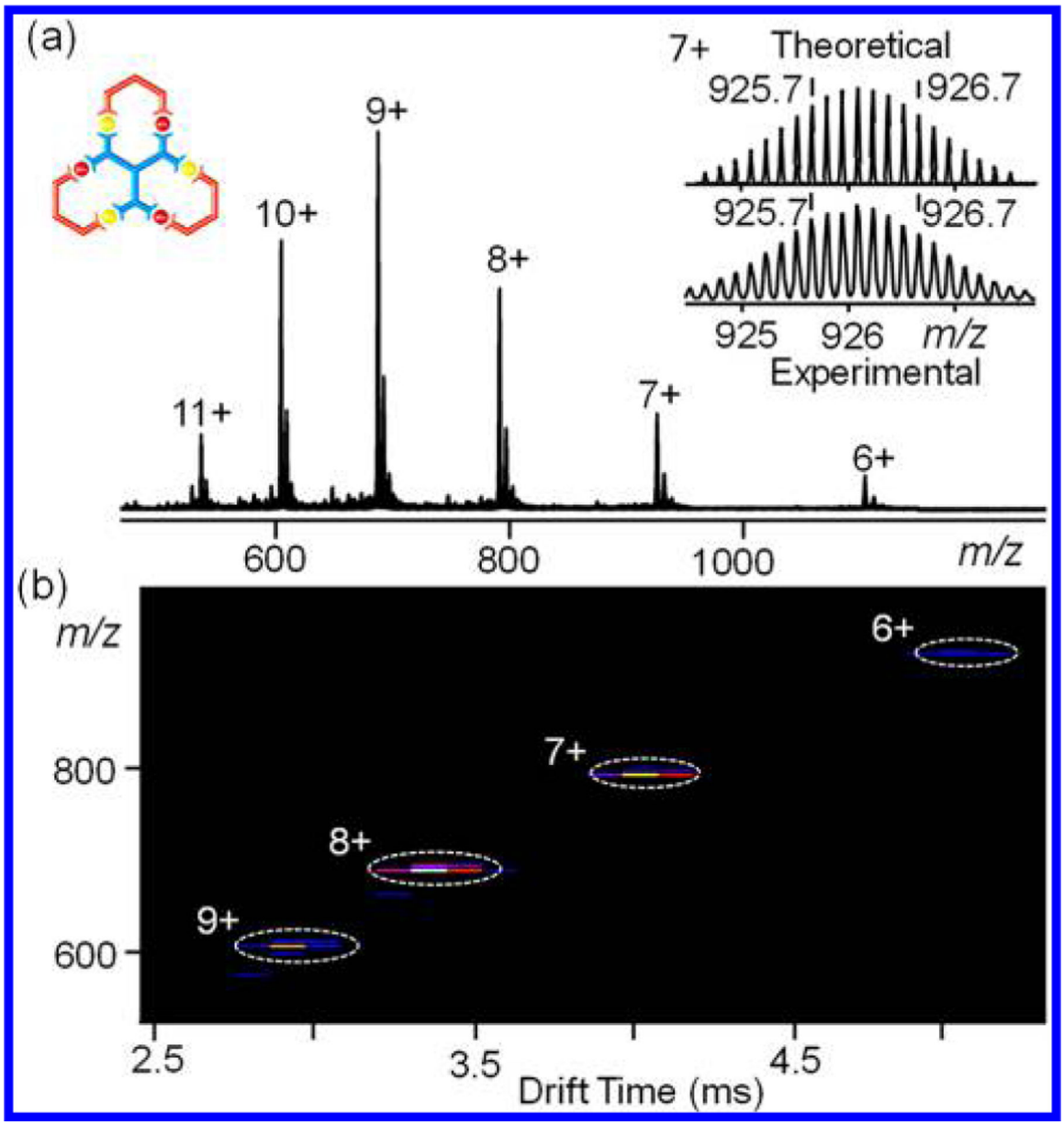

Figure 3.
(a) ESI-MS and (b) TWIM-MS plot (*m/z* vs drift time) of fractal **G2**.

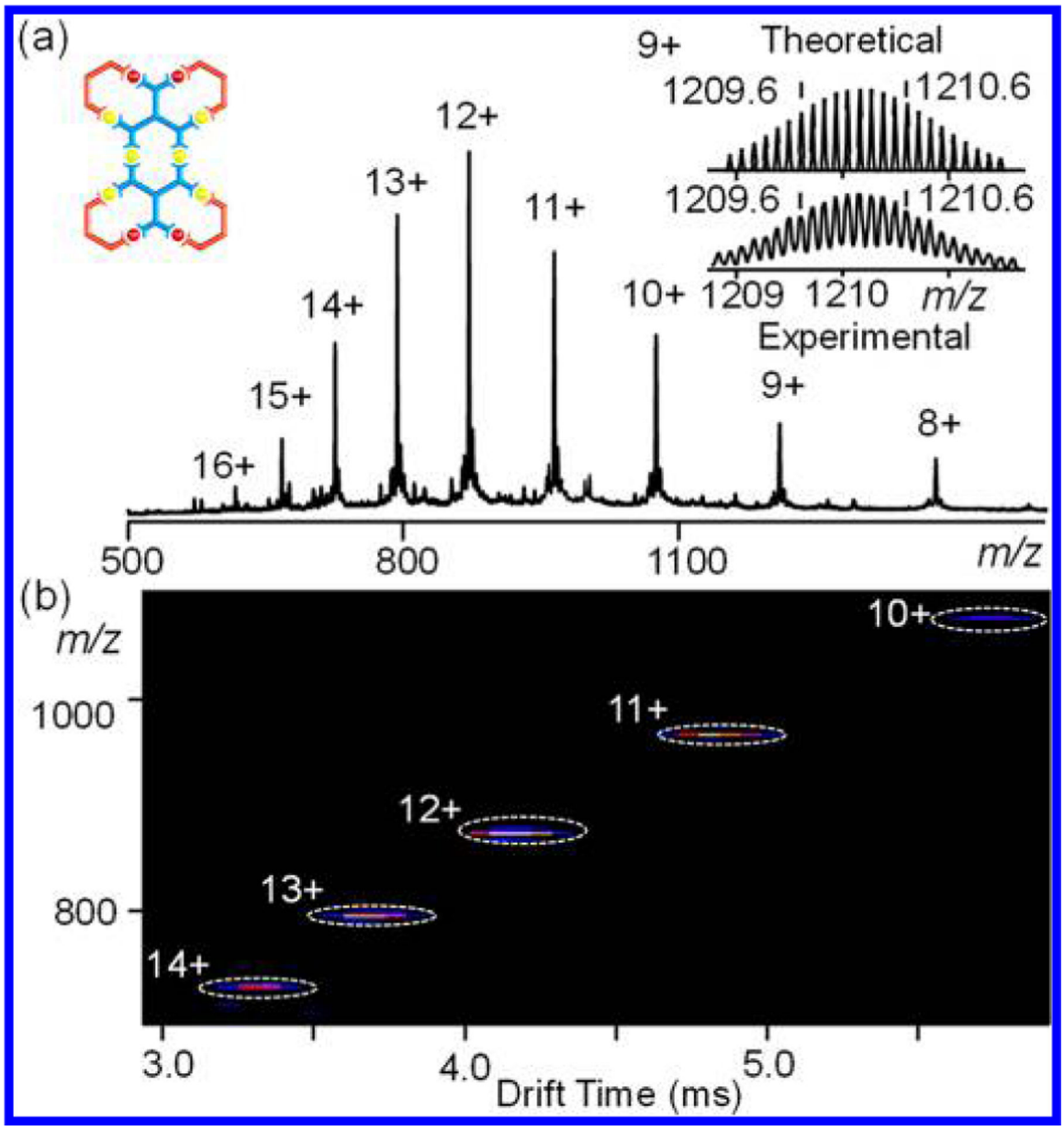

Figure 4.
(a) ESI-MS and (b) TWIM-MS plot (*m/z* vs drift time) of fractal **G3**.

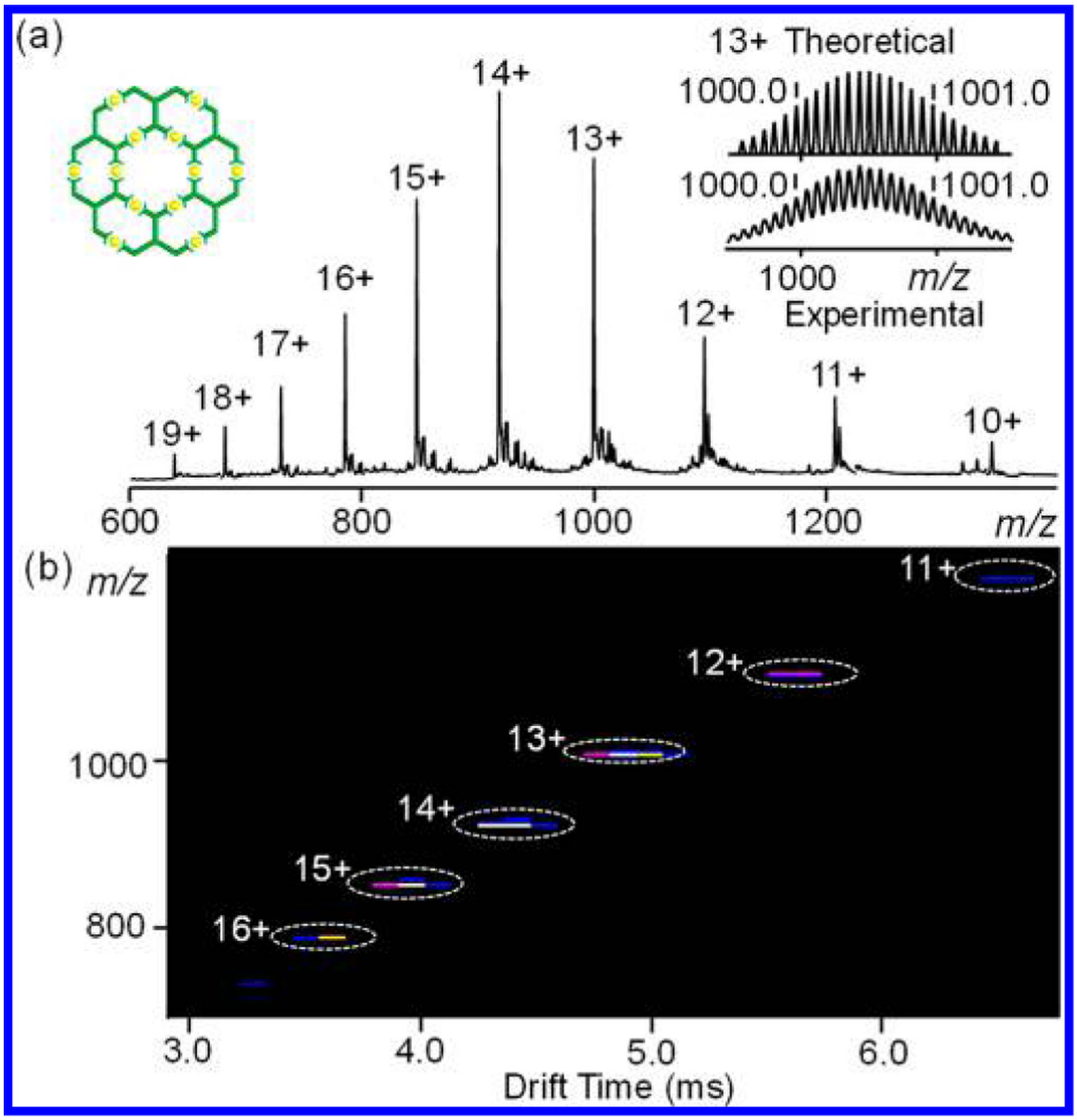

Figure 5.
(a) ESI-MS spectra and (b) TWIM-MS plot (*m/z* vs drift time) of fractal **G4**.

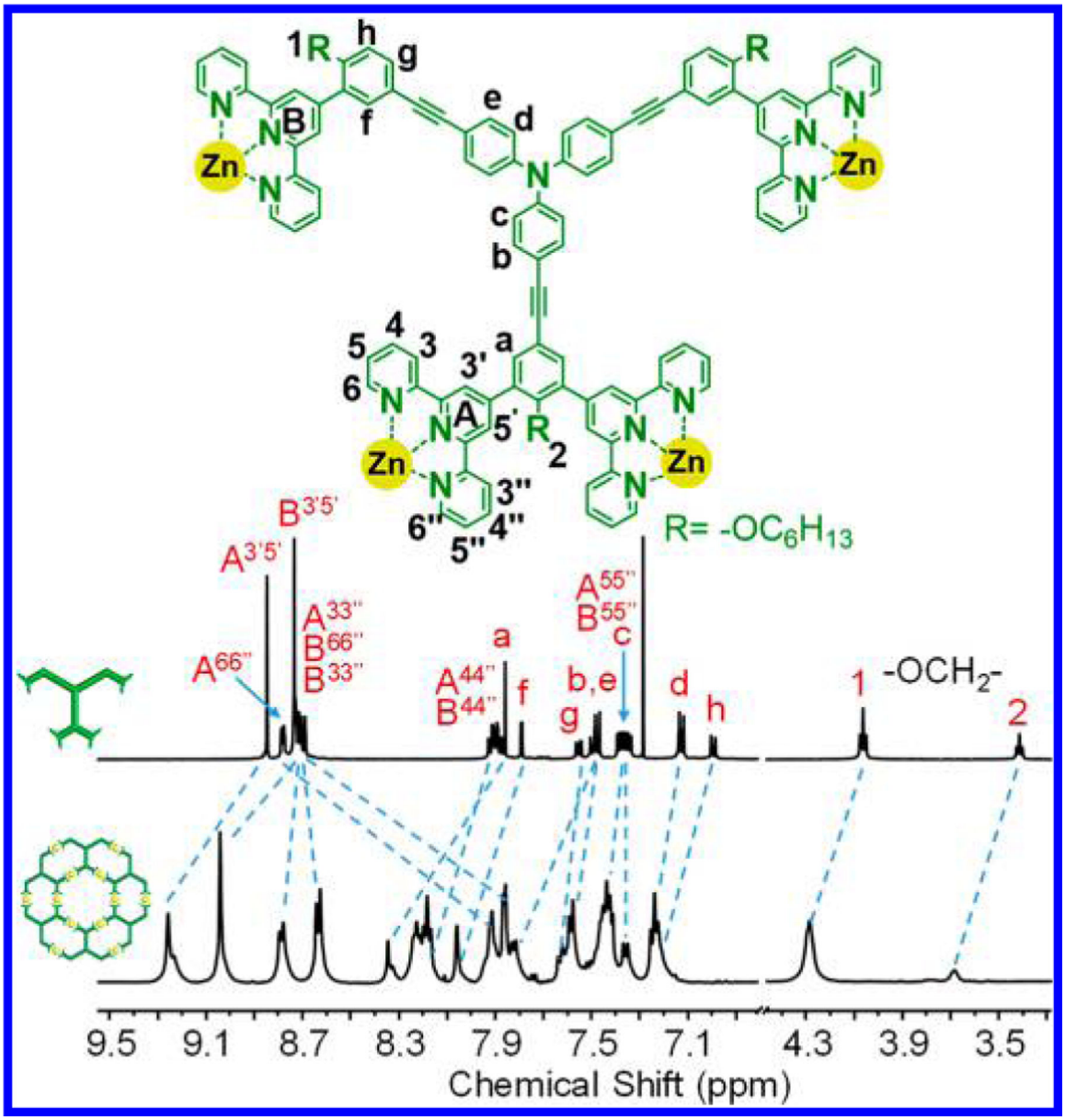

Figure 6.

^{1}H NMR spectra (500 MHz, 300 K) of **LD** in $CDCl_3$ and **G4** in CD_3CN.

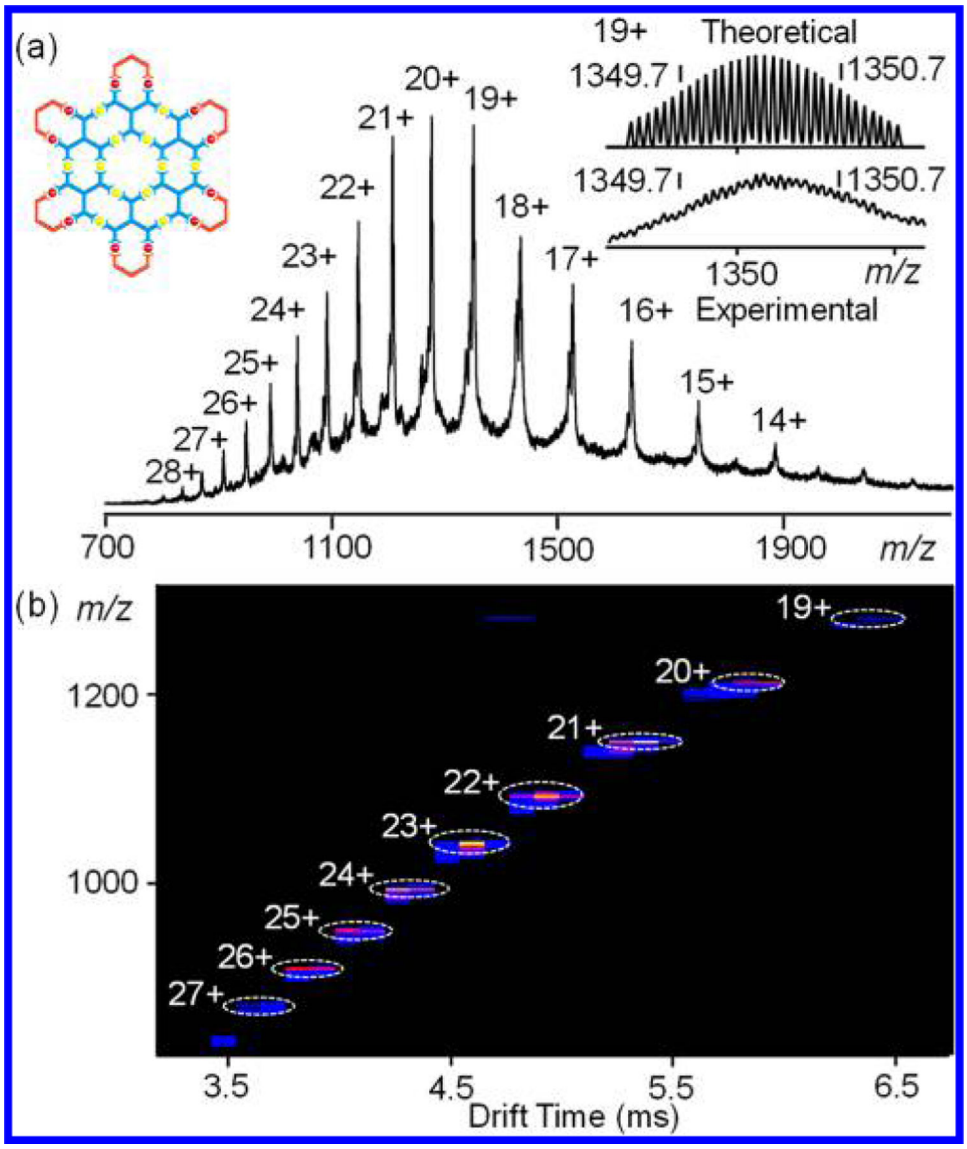

Figure 7.
(a) ESI-MS spectra and (b) TWIM-MS plot (*m/z* vs drift time) of fractal **G5**.

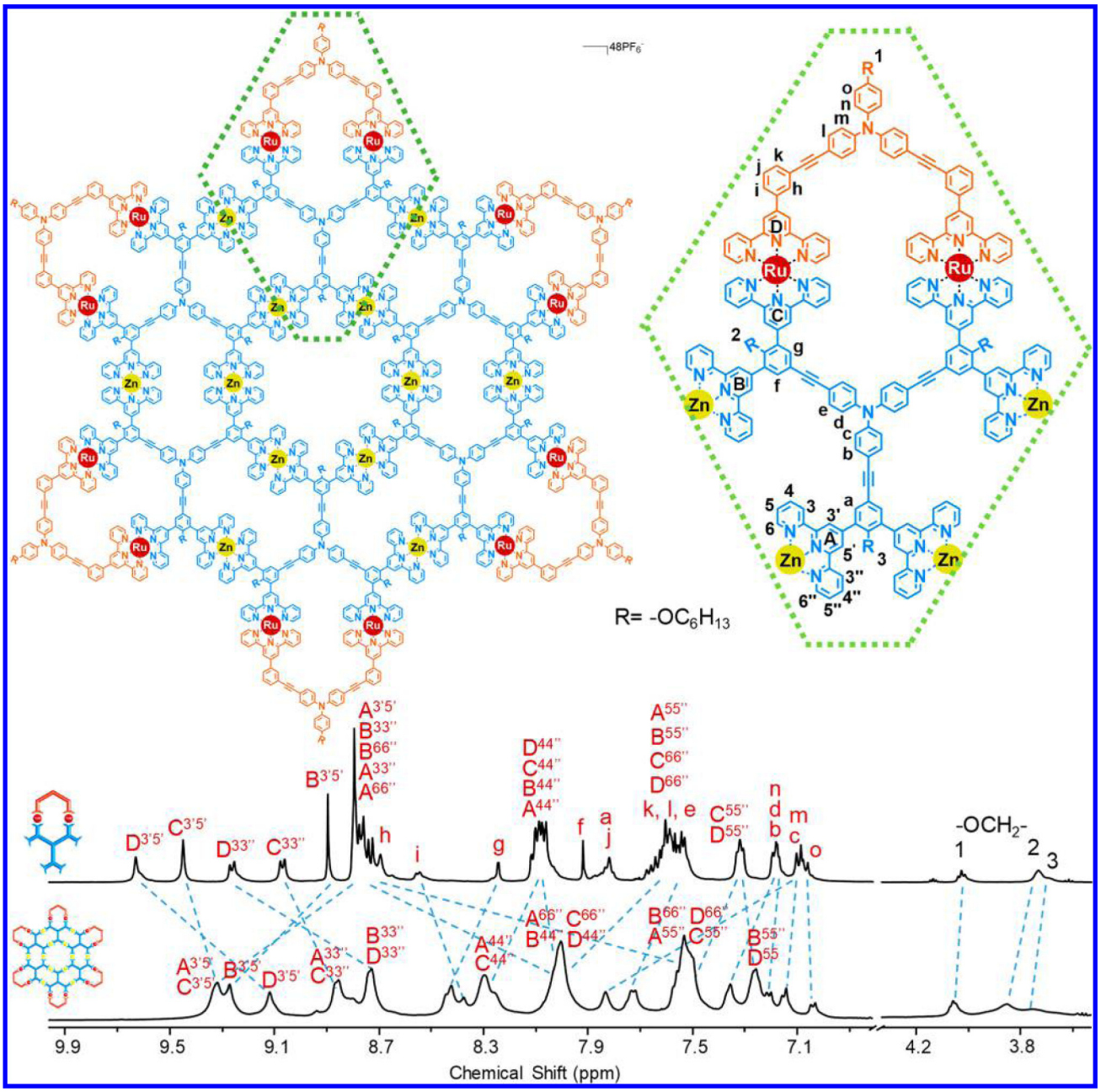

Figure 8.

^{1}H NMR spectra (500 MHz, 300 K) of **LE** in DMSO-d_6 and fractal **G5** in CD_3CN.

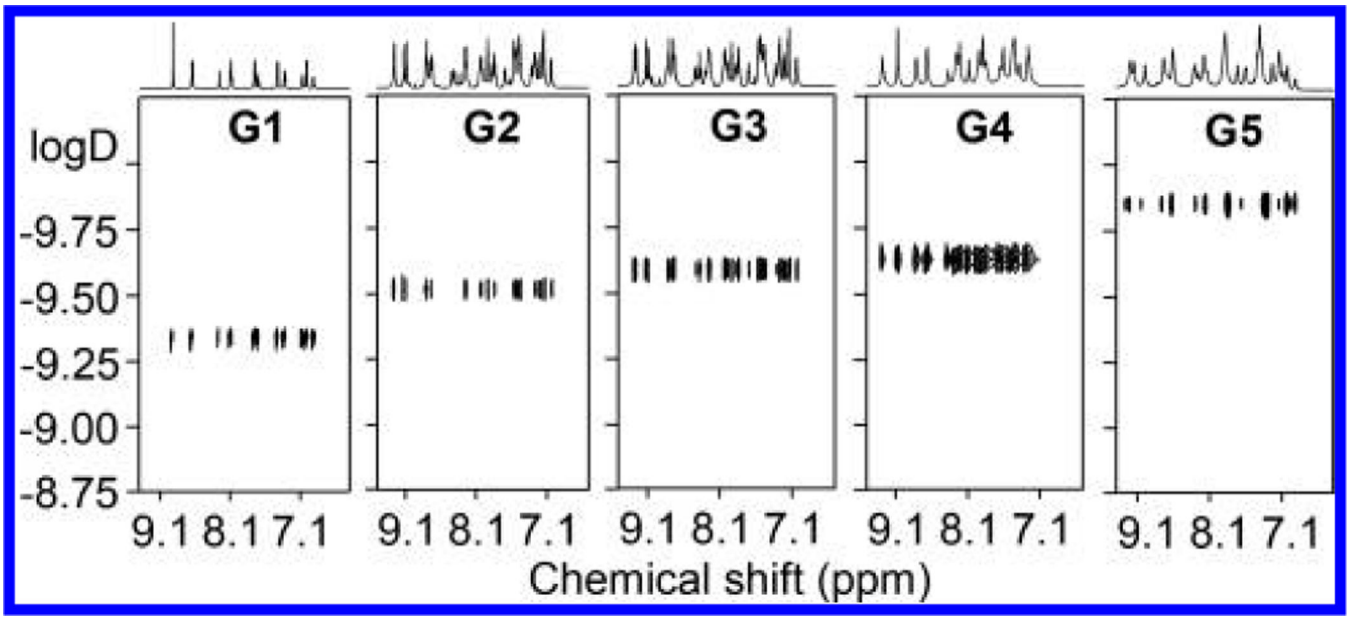

Figure 9.
2D DOSY NMR spectra (600 MHz, 300 K) of **G1−G5** in CD_3CN.

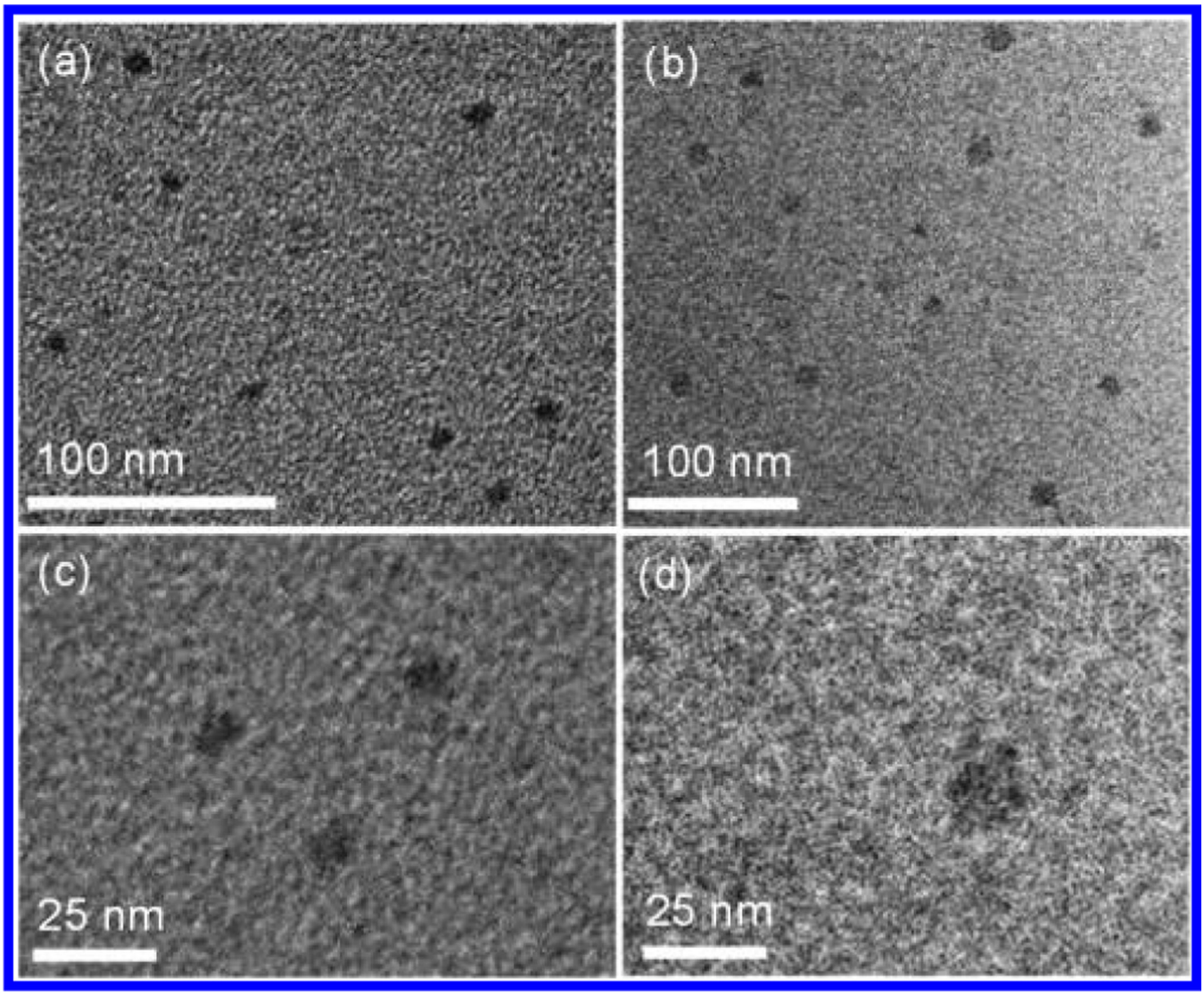

Figure 10.
TEM images of (a,c) **G4** and (b,d) **G5**.

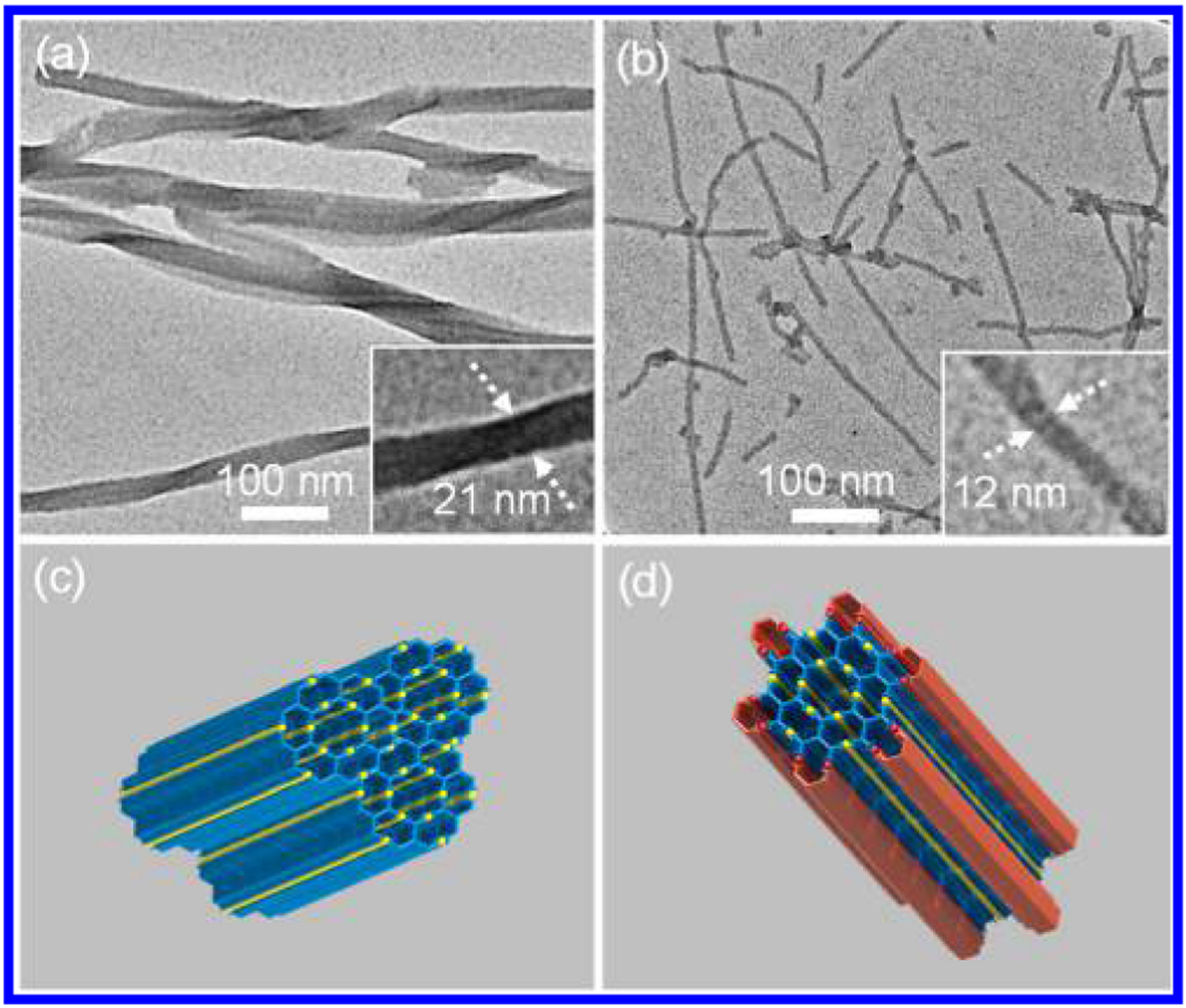

Figure 11.

TEM images of nanostructures formed by (a) **G4** and (b) **G5** in solution and (c,d) proposed packing models (c for **G4**, d for **G5**).

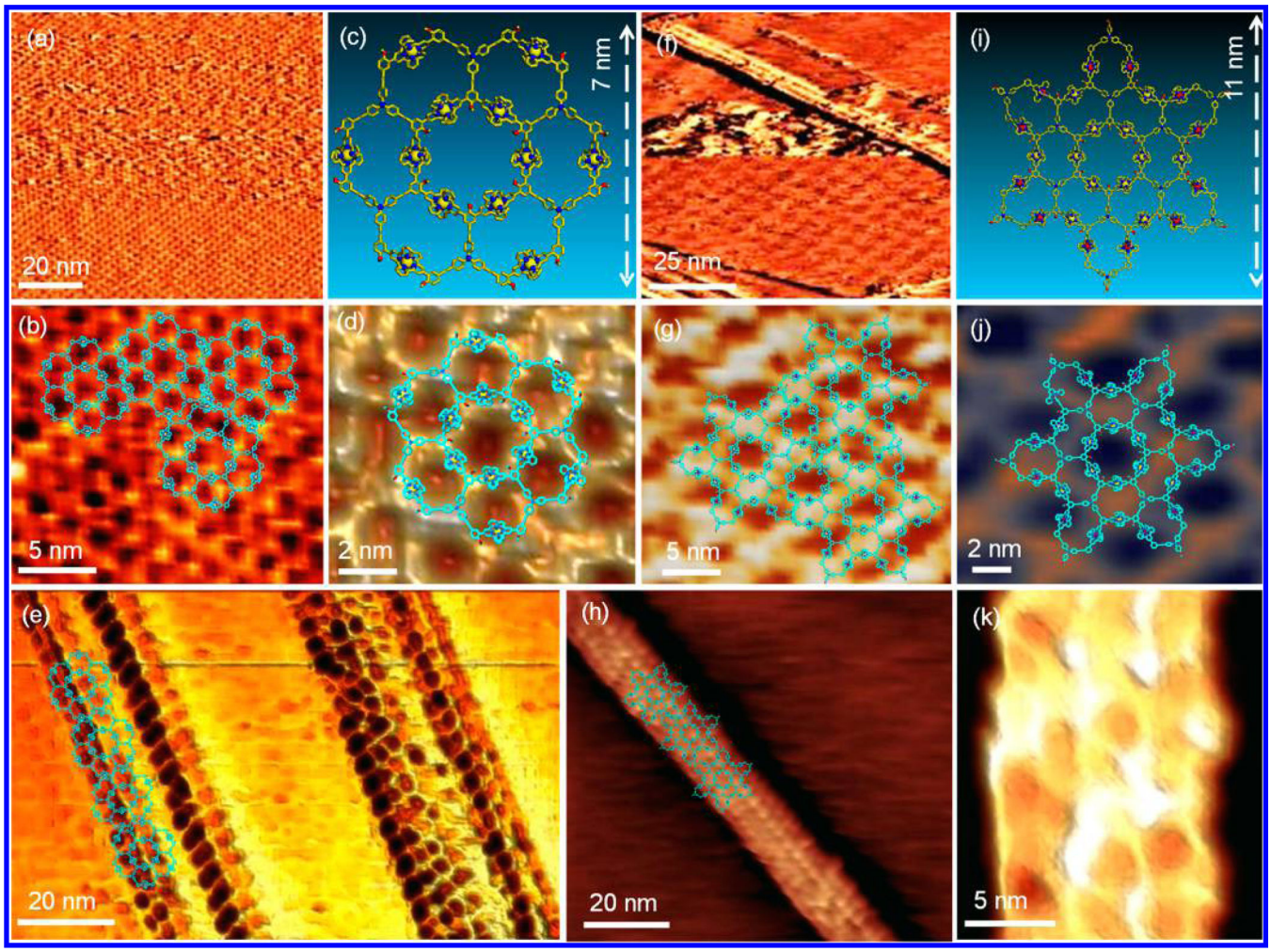

Figure 12.

STM images of 2D networks formed by (a, b, d) **G4** and (f, g, j) **G5**; 1D nanoribbons formed by (e) **G4** and (h, k) **G5** on HOPG (note that d, e, j are 3D STM images); energy-minimized structures for (c) **G4** and (i) **G5**.

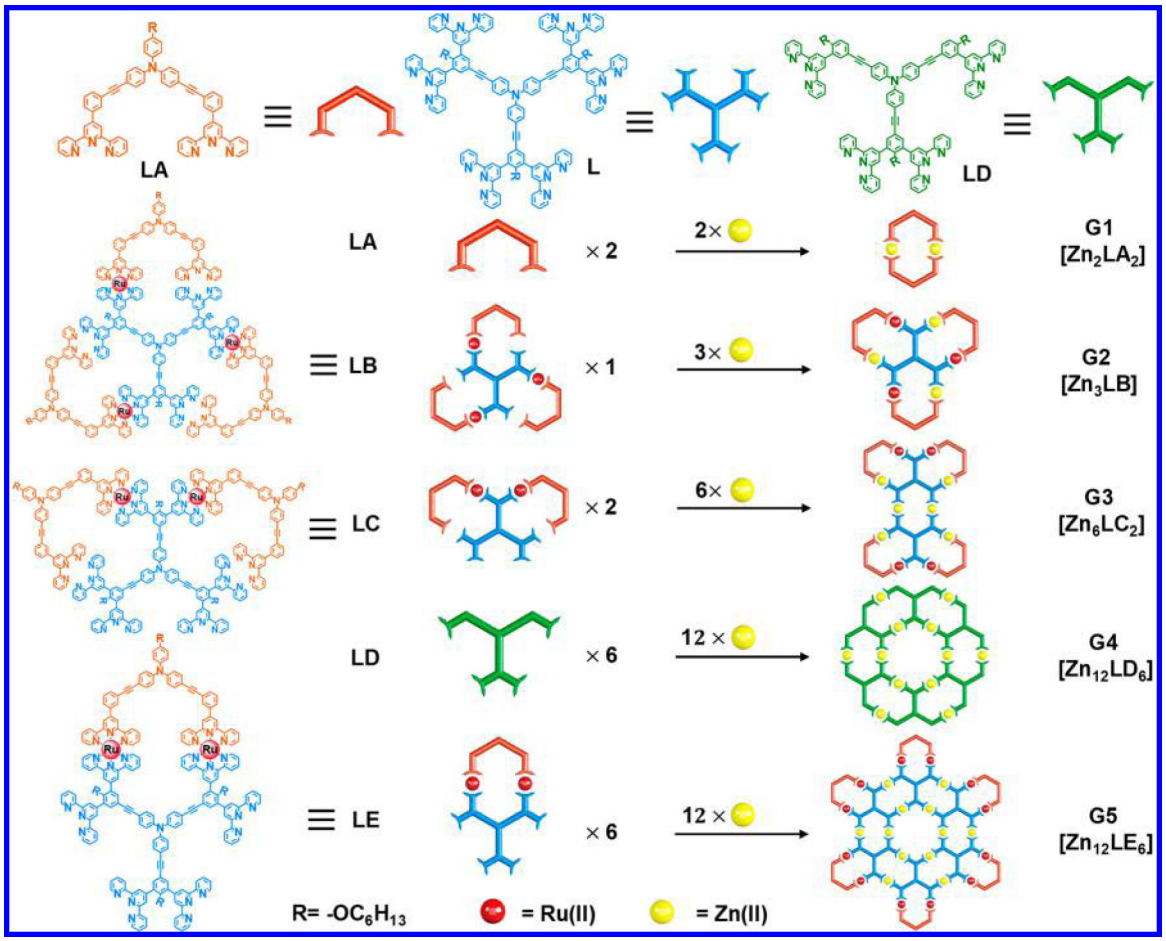

Scheme 1.
Different Approaches to Prepare the Ligands and Fractal Structures

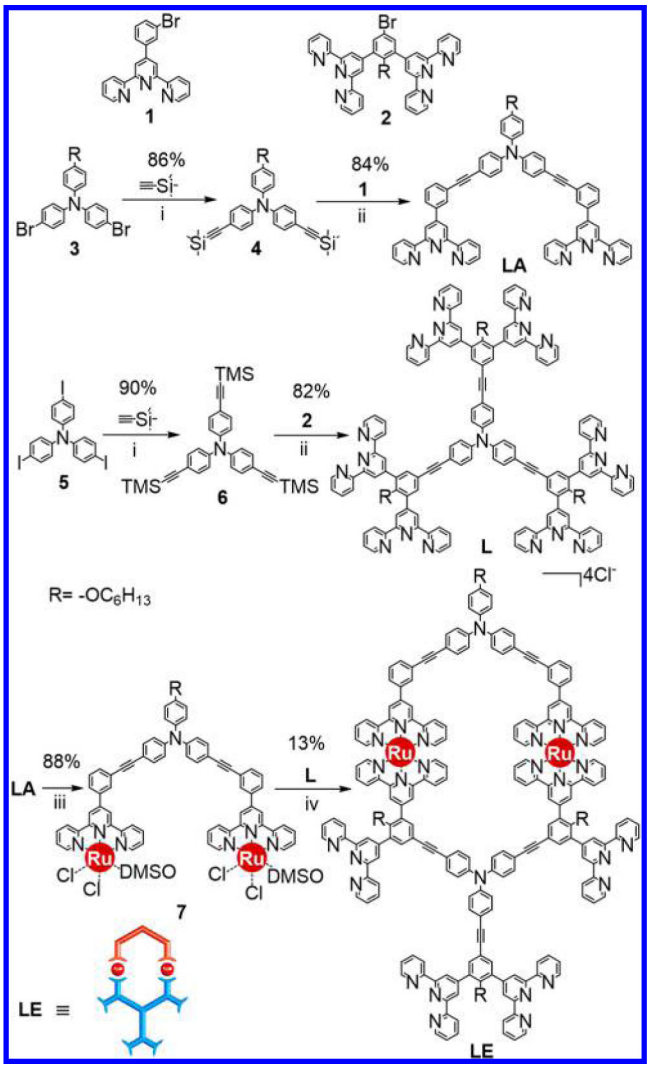

Scheme 2.

Synthesis of ROBB LE[a]

[a](i) $Pd(PPh_3)_2Cl_2$, CuI, THF/Et_3N, 60 °C. (ii) $Pd(PPh_3)_4$, CuI, TBAF, THF/Et_3N, 70 °C. (iii) $Ru(DMSO)_2Cl_2$, 1,2-dichloroethane, 80 °C. (iv) 1,2-dichloroethane/EtOH, 80 °C.